Actively Controllable Solid Phase Microextraction in a Hierarchically Organized Block Copolymer-Nanopore Electrode Array Sensor for Charge-Selective Detection of Bacterial Metabolites

Jin Jia[1†], Seung-Ryong Kwon[2†], Seol Baek[1], Vignesh Sundaresan[3], Tianyuan Cao[1], Allison R. Cutri[1], Kaiyu Fu[4,5], Bridget Roberts[3], Joshua D. Shrout[6,7], Paul W. Bohn[1,3]*

[1] Department of Chemistry and Biochemistry, University of Notre Dame, Notre Dame, Indiana 46556, United States

[2] Department of Chemistry and Research Institute of Natural Science, Gyeongsang National University, Jinju, 52828, South Korea

[3] Department of Chemical and Biomolecular Engineering, University of Notre Dame, Notre Dame, Indiana 46556, United States

[4] Department of Electrical Engineering, Stanford University, Stanford, California 94305, United States

[5] Department of Radiology, Stanford University, Stanford, California 94305, United States

[6] Department of Civil and Environmental Engineering and Earth Sciences, University of Notre Dame, Notre Dame, Indiana 46556, United States

[7] Department of Biological Sciences, University of Notre Dame, Notre Dame, Indiana 46556, United States

[*]Author to whom correspondence should be addressed, *pbohn@nd.edu*.

ABSTRACT

Pseudomonas aeruginosa produces a number of phenazine metabolites, including pyocyanin (PYO), phenazine-1-carboxamide (PCN), and phenazine-1-carboxylic acid (PCA). Among these, PYO has been most widely studied as a biomarker of *P. aeruginosa* infection. However, despite its broad-spectrum antibiotic properties and its role as a precursor in the biosynthetic route leading to other secondary phenazines, PCA has attracted less attention, partially due to its relatively low concentration and interference from other highly abundant phenazines. This challenge is addressed here by constructing a hierarchically organized nanostructure consisting of a pH-responsive block copolymer (BCP) membrane with nanopore electrode arrays (NEAs) filled with gold nanoparticles (AuNPs) to separate and detect PCA in bacterial environments. The BCP@NEA strategy is designed such that adjusting the pH of the bacterial medium to 4.5, which is above the pKa of PCA but below the pKa of PYO and PCN, ensures that PCA is negatively charged and can be selectively transported across the BCP membrane. At pH 4.5, only PCA is transported into the AuNPs-filled NEAs, while PYO and PCN are blocked. Structural characterization illustrates the rigorous spatial segregation of the AuNPs in the NEA nanopore volume, allowing PCA secreted from *P. aeruginosa* to be quantitatively determined as a function of incubation time using square-wave voltammetry and surface-enhanced Raman spectroscopy. The strategy proposed in this study can be extended by changing the nature of the hydrophilic block and subsequently applied to detect other redox-active metabolites at low concentration in complex biological samples and, thus, help understand metabolism in microbial communities.

KEYWORDS

biofilm, square wave voltammetry, SERS, *Pseudomonas aeruginosa*, solid phase microextraction, sensor

The bacterium *Pseudomonas aeruginosa* is an opportunistic pathogen that accounted for approximately 32,600 healthcare-associated infections and contributed to 2,700 estimated deaths in the United States in 2017.[1] *P. aeruginosa* is a metabolically diverse microbe that grows readily in many natural and host-associated environments. Phenazines are one variety of the many types of secondary metabolites produced by *P. aeruginosa* under different growth conditions. These phenazines are redox-active pigments that are toxic to many other microbes and enable *P. aeruginosa* to survive in otherwise hostile environments due to the reactive oxygen species (ROS) generation.[2] Furthermore, it has been proposed that phenazines play a role in altering antibiotic susceptibility.[3] Lastly, because of their association with virulence, the phenazines are attractive as biomarkers that might be suitable to identify *P. aeruginosa* infection.[4]

Several *P. aeruginosa* phenazines have been identified, including phenazine-1-carboxylic acid (PCA) which can be derivatized to phenazine-1-carboxamide (PCN), 1-hydroxyphenazine (1-OHP), 5-methylphenazine-1-carboxylic acid (5-MCA), and pyocyanin (PYO).[3-5] PYO is the best-known and most widely studied blue redox-active secondary metabolite within the phenazine family secreted by *P. aeruginosa*.[6, 7] Studies have shown that PYO interferes with cellular respiration, gene expression, electron transport, and energy metabolism in host cells.[8] In addition, the PYO precursor PCA has shown antifungal and antibacterial activities, which are thought to arise from its oxidative activity and inactivation of important proteins in the oxidative stress response.[9] The antagonistic effects and redox transformations of phenazines greatly affect other microbes, and a more complete knowledge about PCA is necessary to understand the behavior of multi-organism assemblies involving *P. aeruginosa*.

The redox-active and Raman-active properties of PCA make electrochemical and Raman characterization ideal for its study.[3, 5, 10, 11] However, directly detecting PCA in bacterial cultures

is challenging, since there are other abundant metabolites, such as PCN and PYO, which interfere with detection of the less-abundant PCA. One straightforward approach would involve isolation of PCA directly from bacterial cultures. However, conventional separation methods to isolate and purify PCA require time-consuming sample pretreatment. High-performance liquid chromatography, free flow electrophoresis, mass spectrometry, and nuclear magnetic resonance spectroscopy have all been employed to detect phenazines due to their high selectivity, but they either require large sample volumes and sample pretreatment, or the instrumentation is expensive.[12-15] Therefore, it would be very useful to develop a low-cost, low-volume, and efficient isolation method to separate PCA from bacterial cultures containing *P. aeruginosa*.

Recently, heterogeneous block copolymer (BCP) membranes have been applied for the separation of species ranging from small ions to proteins, owing to their tunable nanoscale pore size and charge and the ability to produce highly ordered and diverse nanoarchitectures.[16-18] In particular, poly(styrene)-*b*-poly(4-vinyl pyridine), *i.e.*, PS-*b*-P4VP, has attracted considerable attention, because it exhibits pH-responsive and charge-selective dual gating characteristics, and it can be prepared in a variety of structural motifs.[19] For example, Peinemman and co-workers demonstrated size-selective separation of proteins as well as selective separation of similarly sized proteins by exploiting different isoelectric point values of the proteins.[16] More recently, our laboratory demonstrated that PS-*b*-P4VP BCP membranes can be combined with nanopore electrode arrays (NEAs) to achieve pH-gated, charge-selective electrochemical signal amplification of ions transported into NEAs through the hierarchically organized BCP@NEA membrane.[20]

Here, we extend this strategy to selectively collect low concentration, negatively charged PCA (pKa = 4.2) from positively charged PYO (pKa = 4.9) and neutral PCN by adjusting the pH of the

bacterial culture samples to 4.5.[21, 22] In order to enable both electrochemical and SERS dual mode detection, the NEAs are filled with AuNPs to generate a SERS-active volume within the solid phase microextraction architecture. The introduction of a BCP membrane introduces pH-responsive and charge-selective properties capable of effecting the efficient separation of PCA from other phenazine metabolites produced by *P. aeruginosa*, as shown in **Figure 1**. The negatively charged PCA is transported across the anion-permselective PS-*b*-P4VP into the NEA nanopores where it can be detected using square-wave voltammetry (SWV) and surface-enhanced Raman scattering (SERS). This actively controllable, hierarchically-organized solid phase microextraction architecture was then used to assay PCA produced by *P. aeruginosa* grown in planktonic culture. Interestingly, only a negligible amount of PCA was detected at 8 h incubation, but rapid production was observed from 16 h to 24 h. The integration of pH-gated, charge-selective solid-phase microextraction to isolate PCA with electrochemical and SERS detection in a single monolithic nanostructure produces a biosensor which can detect low-abundance metabolites, and the design flexibility makes it possible to extend the range of application by changing the nature of the hydrophilic block, rendering it applicable to the detection of other, *e.g.*, cationic, redox-active metabolites in complex biological samples. The nanoscale integrated, actively controllable structures developed here have the potential to discover new metabolites and pathways involving low-abundance secreted species.

EXPERIMENTAL SECTION

Materials. Poly(styrene)-*b*-poly(4-vinyl pyridine) (P18248-S4VP, 48.4-b-21.3, M_w/M_n = 1.09) was purchased from Polymer Source. Phenazine-1-carboxylic acid was obtained from SynQuest Laboratories. Phenazine-1-carboxamide, pyocyanin, Rhodamine 6G, potassium ferricyanide (III), hexaammineruthenium (III) chloride, potassium chloride, ethyl alcohol (200 proof), gold

nanoparticles (AuNPs) (150 nm), chromium etchant and latex polystyrene beads (1.1 μm) were purchased from Sigma Aldrich. Sylgard 184 silicone Elastomer Kit was obtained from Dow Corning Corporation. Thermal release tape (REVALPHA) was bought from Nitto Denko Corporation. Dulbecco's Phosphate Buffered Saline (DPBS, 1x, without calcium and magnesium) was purchased from Lonza, and silicon wafers were purchased from University Wafer. Deionized (ρ ~ 18.2 MΩ cm, DI) water was prepared using a Milli-Q Gradient water purification system (Millipore). All reagents were used as received without further purification.

Fabrication of the Sensor. A schematic diagram of the fabrication process is given in **Figure S1**. A gold (Au) layer (400 nm) was deposited in an electron-beam vacuum evaporator (Oerlikon 450B evaporator) using 10 nm titanium (Ti) as an adhesion layer. An additional glass (SiO_2) layer (1 μm) was then deposited by the plasma-enhanced chemical vapor deposition system (Unaxis 790 series) using Ti (10 nm) as an adhesion layer. A close-packed monolayer of latex polystyrene (PS) beads (1.1 μm) was transferred onto the SiO_2 surface at an air-water interface by emersing the edge of the wafer through the PS bead layer. Reactive ion etching (RIE) (3 min) in O_2 gas was processed to reduce the bead size to around 950 nm by using an inductive coupled plasma (ICP) reactor (Oerlikon ICP-RIE system). A chromium (Cr) layer (350 nm) was coated as a protective layer on and between the beads. Then, the beads were physically removed in acetone solution by using laundered polyurethane foam swab lab-tips (Berkshire Corp). Finally, RIE (26 min) in O_2 and CF_4 gas was used to etch the SiO_2 between the protective Cr layers to fabricate SiO_2 nanopores. The device was then immersed into Cr etchant (120 s) to remove the remaining Cr layer.

AuNP-containing solution was centrifuged at 10000 rpm for 10 min (RS-200 microcentrifuge, REVSCI). The solvent was decanted and the AuNPs were dispersed in DI water and sonicated for 5 min. This procedure was repeated twice, and the AuNPs were finally resuspended in DI water to

a concentration of 1.44×10^{10} particles mL^{-1}. The AuNPs solution was then drop cast onto the SiO_2 nanopore wafer, air dried in a fume hood, and stored for future use.

A 2% (w:v) poly(styrene)-*b*-poly(4-vinyl pyridine) solution (in dioxane) was drop cast on a pre-cleaned silicon wafer and spin coated at 500 rpm for 1 min. Then, the membrane was immersed in ethanol and incubated for 30 min. After drying with N_2 gas, the membrane was transferred from silicon wafer onto the AuNP-containing SiO_2 nanopore wafer using thermal release tape. The tape was separated and easily peeled off from the wafer after the device was heated on a hot plate (120 ºC) for 10 s leaving the membrane attached to the AuNPs-contained SiO_2 nanopore wafer. SEM images were acquired to confirm the success of each step.

Characterization. Scanning electron microscopy (SEM) analysis was performed using a Helios G4 Ux dual beam SEM/FIB workstation operating at an acceleration voltage of 5 kV for the electron beam and 25 kV for the ion beam. Raman spectroscopy experiments were conducted by using an Alpha 300R confocal Raman microscope (WITec Instruments Corporation). Excitation radiation at 785 nm from a solid-state diode pumped laser was focused and collected through a 40× (NA = 0.6) objective. WITec project 2.1 and MATLAB (Mathworks Inc.) were used to perform initial data analysis. All Raman experiments were repeated on three replicates per sample condition.

A CHI842C or CHI760A electrochemical workstation (CH Instruments, USA) was used for all electrochemical measurements. Typically, the Au layer was used as working electrode in 3-electrode configuration with Pt counter and Ag/AgCl reference electrode. Prior to electrochemical measurements, a poly(dimethylsiloxane) (PDMS) well was mounted onto the nanopore array to contain 100 µL of an electrolyte solution or bacteria growth medium. SWV experiments were conducted using a potential amplitude of 25 mV and a potential increment of 4 mV at a frequency

of 15 Hz and cyclic voltammograms were obtained at a scan rate of 0.1 V s^{-1}. For the Raman and electrochemical measurements on planktonic culture, the bacteria-free supernatant solution was adjusted to pH 4.5 using hydrochloric acid (1%). The supernatant (pH 4.5) was then transferred onto the device and incubated for 30 min to allow membrane equilibration with the pH 4.5 solution before testing.

Analysis of the SERS Performance of AuNP-filled SiO_2 Nanopores. Rhodamine 6G (10 mM) water solution was drop cast onto a gold-coated silicon wafer and also onto a AuNP-filled BCP@NEA wafer. SERS spectra were recorded under excitation with 785 nm laser as shown in **Figure S2**. Raman enhancement factor (EF) of the AuNPs-containing BCP@NEA structure was calculated from the following equation:

$$EF = (I_{SERS}/N_{SERS})/(I_{Raman}/N_{Bulk})$$

where N_{SERS} and N_{Bulk} represent the number of molecules on the substrate surface and in the bulk solution in the probe volume, respectively, and I_{SERS} and I_{Raman} represent the intensities in SERS and Raman, respectively. N_{SERS} was estimated from the molecular density of a compact monolayer of Rhodamine 6G on half of a monolayer of AuNPs, to account for the fact that AuNPs are thick enough to block incident laser radiation from the backward facing hemisphere, meaning that only half of the AuNP surface was effectively irradiated. I_{SERS} and I_{Raman} were determined from the peak intensities of the band of Rhodamine 6G at ~1595 cm^{-1} and yielded an EF of 1.3×10^5.

Supernatant of Planktonic Culture. P. aeruginosa strain PA14 and its isogenic Δ*phz* (phenazine-null) strain were used in this study.[23] Bacteria were streaked on Luria-Bertani (LB) agar plates and incubated at 37 °C for 16 h. A single colony was inoculated in 10 mL LB medium grown at 37 °C with shaking at 240 rpm. The optical density at 600 nm, OD_{600}, of the *P. aeruginosa* culture was measured to monitor the bacterial growth as shown in **Figure S3**. The bacterial culture was

collected and centrifuged at 15000 rpm for 5 min. The supernatant was filtered (0.2 μm filter pore size) and this bacterial-free supernatant was collected for future use.

Detection of PCA in planktonic culture. The bacteria-free supernatant (0.5 mL) was mixed with chloroform (1 mL), vortexed for 30 s and incubated for another 20 min. After allowing chloroform to settle to the bottom, this phase became green-blue. The aqueous phase was removed. The phenazines were recovered by air-drying the solvent in a fume hood, after which the analytes were redispersed in DI water (pH 4.5). The solution (pH 4.5) was drop cast on the device and incubated for 30 min before testing. Because it was difficult to completely remove all PCA from the device after a measurement cycle, all devices were used for single measurements only.

RESULTS AND DISCUSSION

Functional overview of electrochemical SERS sensor design. The fabrication of the electrochemical SERS sensor is described in the Experimental Section and is shown in **Figure S1**. The resulting AuNP-filled BCP@NEA structures were characterized with SEM imaging. As shown in **Figure 2**, 150 nm AuNPs occupied the majority of the nanopore volume after filling, and the physical integrity of the BCP membrane is clearly evident in **Figures 2A** and **2B** (top- and tilted-view, respectively). The AuNP filling of a typical nanopore is shown in a cross-sectional image in **Figure 2C**. At pH 7.0, above the pKa of the P4VP block (pKa = 4.8), the BCP membrane is hydrophobic and dewetted, and thus no mass transport, including water, occurs, as depicted schematically in **Figure 1B**. However, at pH 4.5, below the P4VP pKa, the P4VP domains of the BCP membrane become protonated, rendering them positively charged, hydrophilic, and anion permselective, permitting negatively charged molecules to pass, as shown in **Figure 1C**.[20] These properties of the BCP portion of the BCP@NEA make it possible to separate molecules based on charge and thus to be used for actively-controllable solid phase micro-extraction. This is

particularly useful in the isolation and detection of PCA, for example. The phenazine biosynthetic pathway in **Figure 1A** shows PCA and four other important metabolites secreted by *P. aeruginosa*. Among them, PYO is the dominant secreted factor in planktonic culture, which makes the other phenazines difficult to detect. However, because the phenazines exhibit pH-dependent charge states, PCA can be isolated by careful manipulation of the charge state of the P4VP domain of the BCP membrane.

Electrochemical characterization of AuNP-filled NEAs. Before attaching the BCP membrane onto the AuNP-filled NEAs, the electrochemical function of the NEAs was characterized by comparing the cyclic voltammetry (CV) of the reversible redox couple, $Fe(CN)_6^{3/4-}$ at 1 mM on AuNP-filled NEAs and a planar gold electrode, as shown in **Figure S4**. The AuNP-filled NEAs produce slightly greater cathodic and anodic peak currents, an observation likely due to the larger active electrode area of AuNP-filled NEAs. Importantly, filling AuNPs into NEA nanopores does not alter the qualitative characteristics of the electrochemical response of $Fe(CN)_6^{3-}$, but the resulting physical architecture has the potential to significantly enhance Raman scattering signals by generating SERS hot spots between AuNPs, thereby enabling simultaneous electrochemical/SERS dual detection of phenazine metabolites.

Selective electrochemical detection of PCA on BCP-coated planar gold electrode. Initially, the pH-responsive permselective behavior of the PS-*b*-P4VP BCP was characterized on a planar gold electrode by electrochemical detection of phenazine metabolites produced by *P. aeruginosa*. As shown in **Figure S5A**, single phenazine species, *i.e.*, PCA, PCN, and PYO, at pH 4.5 in LB medium all generate a distinct peak current in oxidative square wave voltammetry (SWV). However, the three peaks partially overlap in the potential range *ca.* -0.36 V $\leqslant E_{appl} \leqslant$ -0.1 V. Different peak currents for the three phenazines tested suggest that each species exhibits different

electrochemical kinetics. In addition, a mixture composed of PCA, PCN, and PYO (each 33.3μM) was also measured by SWV, and consistent with the significant current overlap observed in the individual responses, a single broad peak was obtained, as shown in **Figure S5B**.

In order to characterize anion permselective transport across the PS-*b*-P4VP BCP membrane, a BCP membrane was spin-coated onto a planar gold electrode. The pH of all phenazine-containing LB medium solutions was adjusted to pH 4.5, which is lower than the pKa of PYO (4.9) and PCN, but higher than the pKa of PCA (4.2).[21, 22] When the BCP membrane-coated gold electrode was exposed to PCN and PYO, oxidative SWV showed no current response beyond a broad background, as shown in **Figure S6A,** consistent with the anion permselective BCP membrane preventing transport of neutral/positive PCN and PYO to the electrode. In contrast, anionic PCA (at pH 4.5) produced a peak response resulting from the anion-selective transport properties of the membrane at pH 4.5. In contrast, no current response was obtained from PCA at pH 7.0, consistent with the P4VP domains being in a collapsed, hydrophobic, dewetted state. The membrane permselectivity exhibited in these planar gold experiments mimics the designed pH-dependent selectivity for PCA on AuNP-filled BCP@NEA structures.

Clearly there is a range of pH over which the desired permselectivity can be obtained. For instance, if pH 4.7 is chosen, it is advantageous in terms of the ionization percentage of PCA, but pH 4.7 being close to the P4VP pKa would diminish the anion permselectivity of the BCP membrane. On the other hand, at pH 4.3, the ionized fraction of PCA is lower, leading to less efficient PCA collection. Thus, pH 4.5 was chosen as a compromise.

Electrochemical quantitation of P. aeruginosa-derived PCA. Next, the BCP membrane was combined with AuNP-filled NEAs for quantitation of PCA secreted by *P. aeruginosa*. **Figure 3A** shows the oxidative SWVs obtained from -0.8 V to +0.2 V *vs.* Ag/AgCl from PCA standards at

varying concentration in LB medium at pH 4.5. To generate a calibration curve, peak current was integrated using the peak finding function on the CHI potentiostat software, which showed a linear relationship with PCA concentration in the range 1 μM ⩽ [PCA] ⩽ 100 μM. The 3.3σ/S limit of detection (LOD) was estimated to be 3.3 μM, which is comparable with other reported LOD values of phenazine metabolites obtained by electrochemical techniques including those obtained by SWV, CV, and differential pulse voltammetry.[6, 24-27]

Next, PCA produced by *P. aeruginosa* in planktonic culture was directly monitored as a function of time from 0 to 24 h at 8 h increments. Before transferring bacteria-free supernatant onto the BCP-coated AuNP-filled NEAs, the growth medium was adjusted to pH 4.5 to ensure that the PCA was net negatively charged. As shown in **Figure 3B**, no PCA was detected in the 0-8 h incubation window, but a distinct peak was observed at 16 h that further increased in intensity at 24 h. PCA concentration was determined to be 36.8 μM and 56.8 μM at 16 and 24 h incubation time, respectively, based on the calibration curve in **Figure 3C**. Samples obtained from an equivalently cultured *P. aeruginosa* Δ*phz* null mutant strain (that cannot produce phenazines) yielded no detectable phenazine signal by SWV on AuNP-filled BCP@NEA structures, thus serving as a biological negative control (**Figure S7**).

SERS detection of PCA. In order to explore the possibility that the BCP@NEA structures could support simultaneous electrochemical and SERS dual detection, SERS spectra were collected at varying concentrations of PCA ranging from 100 nM up to 100 μM at pH 4.5 with 785 nm laser excitation for quantitation, as shown in **Figure 4A**. **Figure 4C** shows that within the PCA concentration ranging from 1 μM to 100 μM, PCA concentration can be expressed quantitatively by $I = 331 \ln C - 104$ ($R^2 = 0.95$), where I is the SERS intensity obtained at 1396 cm^{-1}, and C is the PCA concentration (in μM). The BCP@NEA structure was immersed in the PCA solution for

ca. 30 min to ensure that the P4VP domains in the BCP membrane were hydrophilic and positively charged before SERS analysis. Since the pH-responsive and charge-selective BCP membrane can separate PCA from other more abundant phenazines by selective transport into the BCP@NEA nanopores, the PCA produced by *P. aeruginosa* bacteria can be isolated from the background interferents and selectively detected. To avoid the strong interference from LB medium, the organic metabolites produced in *P. aeruginosa* culture were extracted and redispersed in DI water (at pH 4.5), as shown in **Figure S8** (see Experimental Section for detailed procedure). **Figure 4B** shows the SERS spectra of the samples extracted from PA14 culture at 0, 8, 16, and 24 h incubation times. Importantly, the SERS spectra obtained at 16 h and 24 h are identical to those obtained with commercial PCA but do not match any of the other phenazines (**Figure S9 and Table S1**), confirming the presence of PCA after 16 h incubation with an OD_{600} of 2.0 as isolated by permselective transport into the BCP@NEA structure. Based on the calibration curve, the PCA concentration in *P. aeruginosa* culture was determined to be 3.6 μM and 15.4 μM at 16 and 24 h, respectively, as shown in **Figure 4D**. No PCA was detected in the extracted samples at 0 or 8 h incubation, consistent with the electrochemical results. It is notable that the PCA concentrations measured from the SERS spectra are smaller than those measured with oxidative SWV, a result which can be attributed to mass loss during the extraction process. SERS measurements were also performed for the Δ*phz* mutant and no phenazine signal was detected, as expected, consistent with the SWV results for the Δ*phz* mutant.

CONCLUSIONS

Actively controllable hierarchically organized block copolymer nanopore electrode arrays have been developed to couple solid-phase microextraction with electrochemical and SERS dual-mode sensing. As a model system to demonstrate the capabilities of this approach, the low-abundance

metabolite PCA, produced by *P. aeruginosa*, was measured in the presence of more abundant phenazine metabolites such as PYO and PCN. To fabricate the structure, single gold layer-embedded nanopores are filled with 150 nm AuNPs, to support simultaneous electrochemical and SERS detection. Then, a pH-responsive, charge-selective PS-*b*-P4VP BCP membrane is introduced as a covering layer on the AuNP-filled NEA. The anion permselective PS-*b*-P4VP BCP serves to isolate the less-abundant PCA from other more abundant phenazine metabolites. Thus, under the proper pH conditions, PCA can be selectively detected in the NEA without signal interference from the other more abundant phenazine metabolites. Adjusting solution pH to 4.5 was found to create conditions where negatively charged PCA is selectively transported thorough the BCP membrane to the NEA nanopores while neutral/positive PYO and PCN are excluded from the interior of the NEA nanopores. SWV produced a linear working curve from 1 μM to 100 μM PCA with a LOD of 3.3 μM and SERS was able to detect PCA down to 100 nM.

This approach is immediately applicable to the selective detection of specific virulence factors, such as the phenazines, produced by pathogenic bacteria, like *P. aeruginosa*. The actively controllable solid phase microextraction architecture with electrochemical and SERS sensing capabilities was demonstrated by detecting the minor metabolite PCA in the presence of abundant competing phenazine metabolites. Using this monolithic nanoscale isolation/sensing architecture, the production of PCA by PA14 *P. aeruginosa* was followed for 24 h using both SVW and SERS. Both methods returned comparable results, with no PCA detected from 0-8 h, followed by an onset and subsequent rapid production of PCA, producing increasing concentrations at 16-24 h, which is consistent with previous work on phenazine production.[28]

The actively controlled hierarchically-organized solid phase microextraction/sensor can certainly be extended. One simple extension would substitute another polymer for the PS-*b*-P4VP

BCP. Using poly(styrene-*b*-acrylic acid), for example, could produce a cation permselective layer, and manipulation of the polymer side chains would provide an entrée to tuning the pH-sensitivity. These structures could then be used to detect other metabolites produced by microbial communities on-demand. In addition, since SERS and SWV/CV provide complementary molecular information, *e.g.*, quantitative assays of electroactive species from electrochemical measurements and molecular fingerprint information from SERS measurements, the combined isolation/detection capabilities could provide new ways to examine the secreted factors characteristic of metabolic pathways and those regulating the interaction with neighboring organisms in microbial assemblies.

Supporting Information

The Supporting Information is available free of charge. Additional experimental details and characterization, including schematic images of sensor fabrication, SERS/Raman spectra of Rhodamine 6G, growth curve of PA14, electrochemical characterization of BCP membrane and BCP-coated AuNP-filled NEAs, oxidative SWV of Δ*phz* grown in LB medium, preparation of bacteria samples, and Raman spectra of PCN and PYO.

Acknowledgements

The development of the BCP@NEA structures was supported by the National Science Foundation through grant 1904196, and the phenazine sensor development was supported by National Institute of Allergies and Infectious Diseases by grant R01AI113219. The authors gratefully acknowledge Notre Dame Nanofabrication Facility and Integrated Imaging Facility for providing fabrication and characterization support.

Author information

Corresponding Author

*E-mail: pbohn@nd.edu. Tel.: +1 574 631 1849. Fax: +1 574 631 8366.

ORCID

Jin Jia: 0000-0002-2194-5607

Seung-Ryong Kwon: 0000-0002-0890-523X

Seol Baek: 0000-0003-2191-6723

Vignesh Sundaresan: 0000-0001-9390-1681

Tianyuan Cao: 0000-0002-5854-1972

Allison R. Cutri: 0000-0001-6415-3741

Kaiyu Fu: 0000-0002-7899-0388

Bridget Roberts: 0000-0002-4176-7895

Joshua D. Shrout: 0000-0001-9509-2187

Paul W. Bohn: 0000-0001-9052-0349

Author contributions

†Jin Jia and Seung-Ryong Kwon contributed equally to this work.

J.J., S.R.K., J.D.S., and P.W.B. planned the experiments. J.J. and S.R.K. fabricated the device. J.J. prepared bacterial samples and performed SERS experiments. S.R.K., S.B. and J.J. performed the electrochemical experiments. V.S. contributed to SEM characterization. T.Y.C., K.Y.F and B.R. contributed to the SERS data analysis. A.R.C. prepared the substrate of the sensor. J.J., S.R.K., J.D.S., and P.W.B. wrote the manuscript. All authors edited the manuscript.

Competing financial interest: The authors declare no competing financial interest.

References

1. Wilson, G. M.; Fitzpatrick, M.; Walding, K.; Gonzalez, B.; Schweizer, M. L.; Suda, K. J.; Evans, C. T., Meta-analysis of Clinical Outcomes Using Ceftazidime/avibactam, Ceftolozane/tazobactam, and Meropenem/vaborbactam for the Treatment of Multidrug-resistant Gram-negative Infections. *Open Forum Infect. Dis.* **2021,** *8* (2).

2. Fu, T.; Cai, Z.; Yue, Z.; Yang, H.; Fang, B.; Zhang, X.; Fan, Z.; Pan, X.; Yang, F.; Jin, Y.; Cheng, Z.; Wu, W.; Sun, B.; Huigens, R. W.; Yang, L.; Bai, F., Evolution of Resistance to Phenazine Antibiotics in Staphylococcus aureus and Its Role During Coinfection with Pseudomonas aeruginosa. *ACS Infect. Dis.* **2021,** *7* (3), 636-649.

3. Schiessl, K. T.; Hu, F.; Jo, J.; Nazia, S. Z.; Wang, B.; Price-Whelan, A.; Min, W.; Dietrich, L. E. P., Phenazine Production Promotes Antibiotic Tolerance and Metabolic Heterogeneity in Pseudomonas aeruginosa Biofilms. *Nat. Commun.* **2019,** *10* (1), 762.

4. Recinos, D. A.; Sekedat, M. D.; Hernandez, A.; Cohen, T. S.; Sakhtah, H.; Prince, A. S.; Price-Whelan, A.; Dietrich, L. E. P., Redundant Phenazine Operons in Pseudomonas aeruginosa Exhibit Environment-dependent Expression and Differential Roles in Pathogenicity. *Proc. Natl. Acad. Sci. U. S. A.* **2012,** *109* (47), 19420.

5. Bodelón, G.; Montes-García, V.; López-Puente, V.; Hill, E. H.; Hamon, C.; Sanz-Ortiz, M. N.; Rodal-Cedeira, S.; Costas, C.; Celiksoy, S.; Pérez-Juste, I.; Scarabelli, L.; La Porta, A.; Pérez-Juste, J.; Pastoriza-Santos, I.; Liz-Marzán, L. M., Detection and Imaging of Quorum Sensing in Pseudomonas aeruginosa Biofilm Communities by Surface-enhanced Resonance Raman Scattering. *Nat. Mater.* **2016,** *15* (11), 1203-1211.

6. Elliott, J.; Simoska, O.; Karasik, S.; Shear, J. B.; Stevenson, K. J., Transparent Carbon Ultramicroelectrode Arrays for the Electrochemical Detection of a Bacterial Warfare Toxin, Pyocyanin. *Anal. Chem.* **2017,** *89* (12), 6285-6289.

7. Lau, G. W.; Hassett, D. J.; Ran, H.; Kong, F., The Role of Pyocyanin in Pseudomonas aeruginosa Infection. *Trends Mol. Med.* **2004,** *10* (12), 599-606.

8. Rada, B.; Leto, T. L., Pyocyanin Effects on Respiratory Epithelium: Relevance in Pseudomonas aeruginosa Airway Infections. *Trends Microbiol.* **2013,** *21* (2), 73-81.

9. Price-Whelan, A.; Dietrich, L. E. P.; Newman, D. K., Rethinking 'Secondary' Metabolism: Physiological Roles for Phenazine Antibiotics. *Nat. Chem. Biol.* **2006,** *2* (2), 71-78.

10. Dietrich, L. E. P.; Teal, T. K.; Price-Whelan, A.; Newman, D. K., Redox-active Antibiotics Control Gene Expression and Community Behavior in Divergent Bacteria. *Science* **2008,** *321* (5893), 1203.

11. Green, J.; Paget, M. S., Bacterial Redox Sensors. *Nat. Rev. Microbiol.* **2004,** *2* (12), 954-966.

12. Pastells, C.; Pascual, N.; Sanchez-Baeza, F.; Marco, M. P., Immunochemical Determination of Pyocyanin and 1-hydroxyphenazine as Potential Biomarkers of Pseudomonas aeruginosa Infections. *Anal. Chem.* **2016,** *88* (3), 1631-1638.

13. Parsons, J. F.; Song, F.; Parsons, L.; Calabrese, K.; Eisenstein, E.; Ladner, J. E., Structure and Function of the Phenazine Biosynthesis Protein PhzF from Pseudomonas fluorescens 2-79. *Biochemistry* **2004,** *43* (39), 12427-12435.

14. Ahuja, E. G.; Janning, P.; Mentel, M.; Graebsch, A.; Breinbauer, R.; Hiller, W.; Costisella, B.; Thomashow, L. S.; Mavrodi, D. V.; Blankenfeldt, W., PhzA/B Catalyzes the Formation of the Tricycle in Phenazine Biosynthesis. *J. Am. Chem. Soc.* **2008,** *130* (50), 17053-17061.

15. Liu, H.-M.; Zhang, X.-H.; Huang, X.-Q.; Cao, C.-X.; Xu, Y.-Q., Rapid Quantitative Analysis of Phenazine-1-carboxylic Acid and 2-hydroxyphenazine from Fermentation Culture of

Pseudomonas chlororaphis GP72 by Capillary Zone Electrophoresis. *Talanta* **2008,** *76* (2), 276-281.

16. Qiu, X.; Yu, H.; Karunakaran, M.; Pradeep, N.; Nunes, S. P.; Peinemann, K.-V., Selective Separation of Similarly Sized Proteins with Tunable Nanoporous Block Copolymer Membranes. *ACS Nano* **2013,** *7* (1), 768-776.

17. Abetz, V., Isoporous Block Copolymer Membranes. *Macromol. Rapid Commun.* **2015,** *36* (1), 10-22.

18. Stuart, M. A. C.; Huck, W. T. S.; Genzer, J.; Müller, M.; Ober, C.; Stamm, M.; Sukhorukov, G. B.; Szleifer, I.; Tsukruk, V. V.; Urban, M.; Winnik, F.; Zauscher, S.; Luzinov, I.; Minko, S., Emerging Applications of Stimuli-responsive Polymer Materials. *Nat. Mater.* **2010,** *9* (2), 101-113.

19. Yu, H.; Qiu, X.; Nunes, S. P.; Peinemann, K.-V., Biomimetic Block Copolymer Particles with Gated Nanopores and Ultrahigh Protein Sorption Capacity. *Nat. Commun.* **2014,** *5* (1), 4110.

20. Baek, S.; Kwon, S.-R.; Fu, K.; Bohn, P. W., Ion Gating in Nanopore Electrode Arrays with Hierarchically Organized pH-responsive Block Bopolymer Membranes. *ACS Appl. Mater. Interf.* **2020,** *12* (49), 55116-55124.

21. Brisbane, P. G.; Janik, L. J.; Tate, M. E.; Warren, R. F., Revised Structure for the Phenazine Antibiotic from Pseudomonas fluorescens 2-79 (NRRL B-15132). *Antimicrob. Agents Chemother.* **1987,** *31* (12), 1967-1971.

22. Friedheim, E.; Michaelis, L., Potentiometric Study of Pyocyanine. *J. Biol. Chem.* **1931,** *91* (1), 355-368.

23. Do, H.; Kwon, S.-R.; Fu, K.; Morales-Soto, N.; Shrout, J. D.; Bohn, P. W., Electrochemical Surface-enhanced Raman Spectroscopy of Pyocyanin Secreted by Pseudomonas aeruginosa Communities. *Langmuir* **2019,** *35* (21), 7043-7049.

24. Filer, J. E.; Channon, R. B.; Henry, C. S.; Geiss, B. J., A Nuclease Protection ELISA Assay for Colorimetric and Electrochemical Detection of Nucleic Acids. *Analytical Methods* **2019,** *11* (8), 1027-1034.

25. Simoska, O.; Sans, M.; Fitzpatrick, M. D.; Crittenden, C. M.; Eberlin, L. S.; Shear, J. B.; Stevenson, K. J., Real-time Electrochemical Detection of Pseudomonas aeruginosa Phenazine Metabolites Using Transparent Carbon Ultramicroelectrode Arrays. *ACS Sensors* **2019,** *4* (1), 170-179.

26. Alatraktchi, F. A. a.; Johansen, H. K.; Molin, S.; Svendsen, W. E., Electrochemical Sensing of Biomarker for Diagnostics of Bacteria-specific Infections. *Nanomedicine* **2016,** *11* (16), 2185-2195.

27. Simoska, O.; Sans, M.; Eberlin, L. S.; Shear, J. B.; Stevenson, K. J., Electrochemical Monitoring of the Impact of Polymicrobial Infections on Pseudomonas aeruginosa and Growth Dependent Medium. *Biosens. Bioelectron.* **2019,** *142*, 111538.

28. Do, H.; Kwon, S.-R.; Baek, S.; Madukoma, C. S.; Smiley, M. K.; Dietrich, L. E.; Shrout, J. D.; Bohn, P. W., Redox Cycling-based Detection of Phenazine Metabolites Secreted from Pseudomonas aeruginosa in Nanopore Electrode Arrays. *Analyst* **2021,** *146* (4), 1346-1354.

29. Bellin, D. L.; Sakhtah, H.; Rosenstein, J. K.; Levine, P. M.; Thimot, J.; Emmett, K.; Dietrich, L. E. P.; Shepard, K. L., Integrated Circuit-based Electrochemical Sensor for Spatially Resolved Detection of Redox-active Metabolites in Biofilms. *Nat. Commun.* **2014,** *5* (1), 3256.

30. Bellin, D. L.; Sakhtah, H.; Zhang, Y.; Price-Whelan, A.; Dietrich, L. E. P.; Shepard, K. L., Electrochemical Camera Chip for Simultaneous Imaging of Multiple Metabolites in Biofilms. *Nat. Commun.* **2016,** *7* (1), 10535.

31. Clifford, E. R.; Bradley, R. W.; Wey, L. T.; Lawrence, J. M.; Chen, X.; Howe, C. J.; Zhang, J. Z., Phenazines As Model Low-midpoint Potential Electron Shuttles for Photosynthetic Bioelectrochemical Systems. *Chem. Sci.* **2021,** *12* (9), 3328-3338.

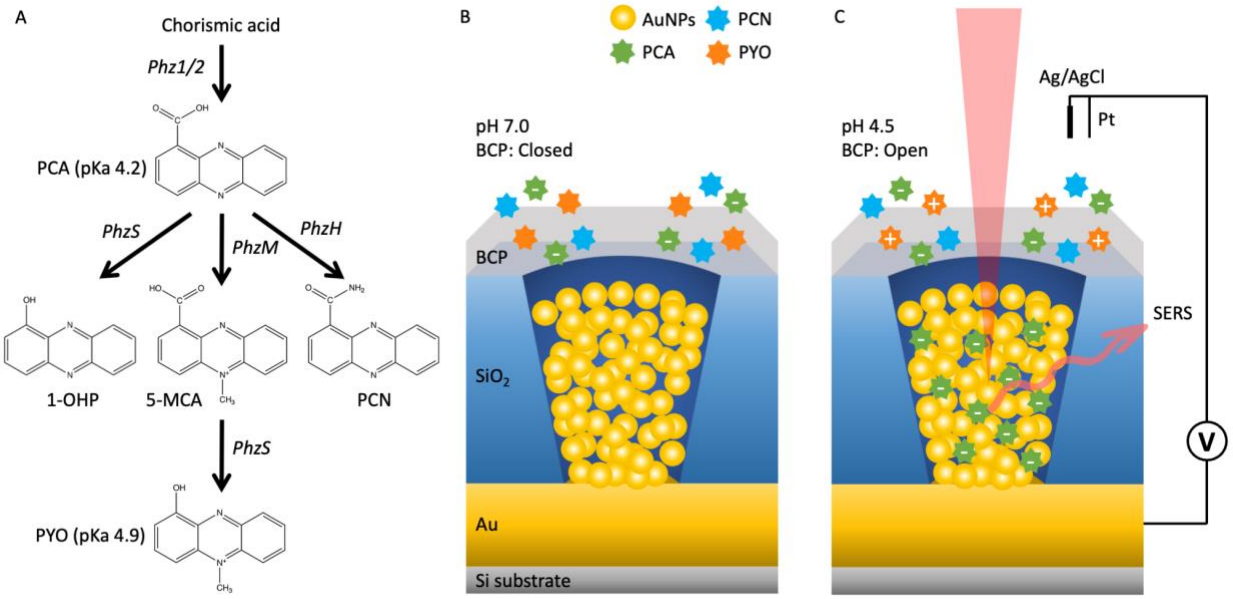

Figure 1. Architecture and scheme of the hierarchically-organized BCP@NEA electrochemical SERS sensor. (A) Phenazine biosynthetic pathway in *P. aeruginosa*. PCA, phenazine-1-carboxylic acid; 1-OHP, 1-hydroxyphenazine; 5-MCA, 5-methylphenazine-1-carboxylic acid; PCN, phenazine-1-carboxamide; PYO, pyocyanin. Phenazine-modifying genes for the conversion reactions are labelled along with arrows.[5, 29-31] (B) Schematic illustration of the electrochemical SERS sensor with BCP gate closed at pH 7.0. (C) Schematic illustration of the electrochemical SERS sensor with BCP gate open at pH 4.5 for the permselective transport and detection of negatively charged molecules by square wave voltammetry and SERS.

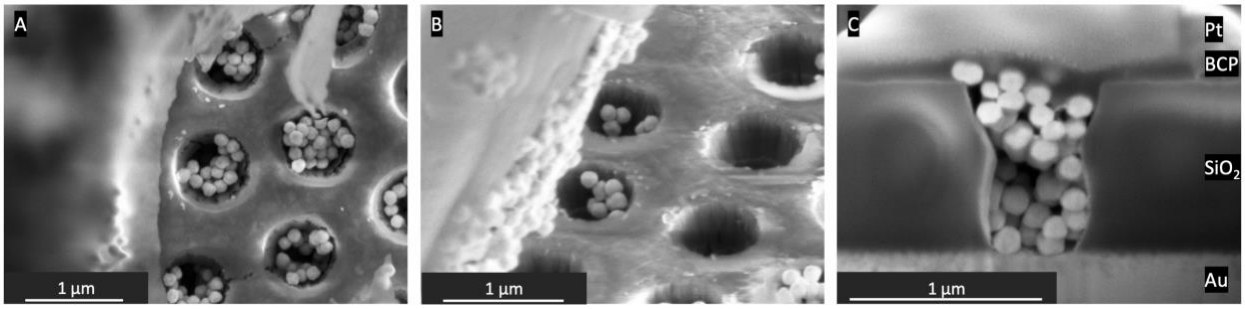

Figure 2. Scanning electron microscopy (SEM) images of the hierarchically-organized BCP@NEA electrochemical SERS sensor. Top-view (A) and tilted-view (B) SEM images of the electrochemical SERS sensor showing membrane-covered (left side of both A and B) and uncovered (right side of both A and B) NEA with AuNPs. (C) Cross-sectional SEM image of a single Au nanoparticle-filled nanopore from the sensor.

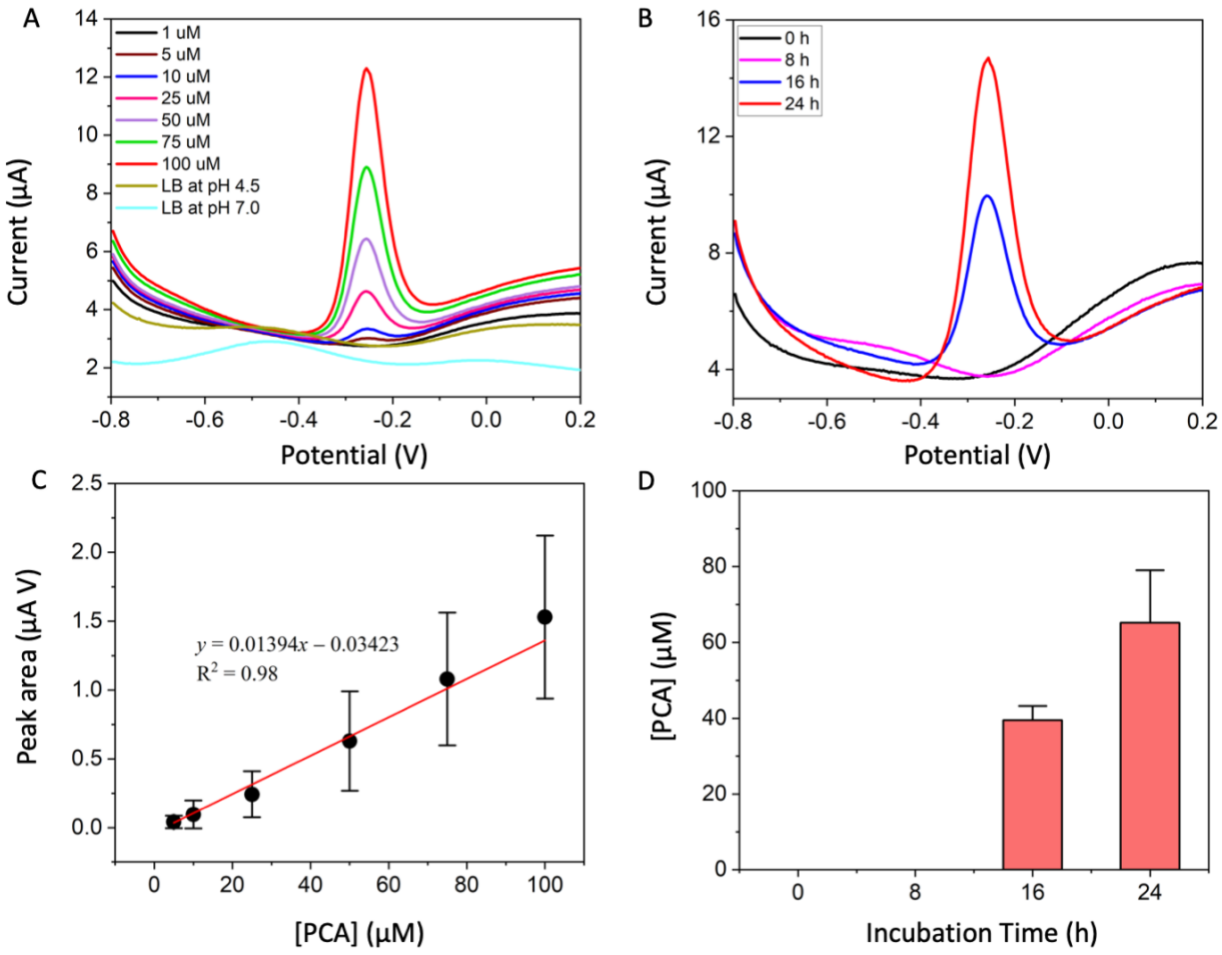

Figure 3. Electrochemical detection of PCA. (A) Representative oxidative SWVs as a function of PCA concentration ranging from 1 μM to 100 μM in LB medium at pH 4.5. (B) Oxidative SWVs obtained at different incubation times from *P. aeruginosa* cultured in LB medium. Prior to electrochemical detection, the collected sample was adjusted to pH 4.5 for the selective separation and transport of PCA into the interior of the BCP@NEAs. (C) The calibration plot for peak SWV current *vs*. PCA concentration. The mean values and standard deviations were calculated from three independent measurements. (D) Histograms of the measured concentration of PCA secreted from *P. aeruginosa* based on the PCA calibration plots. The error bars indicate standard deviation obtained from three independent measurements.

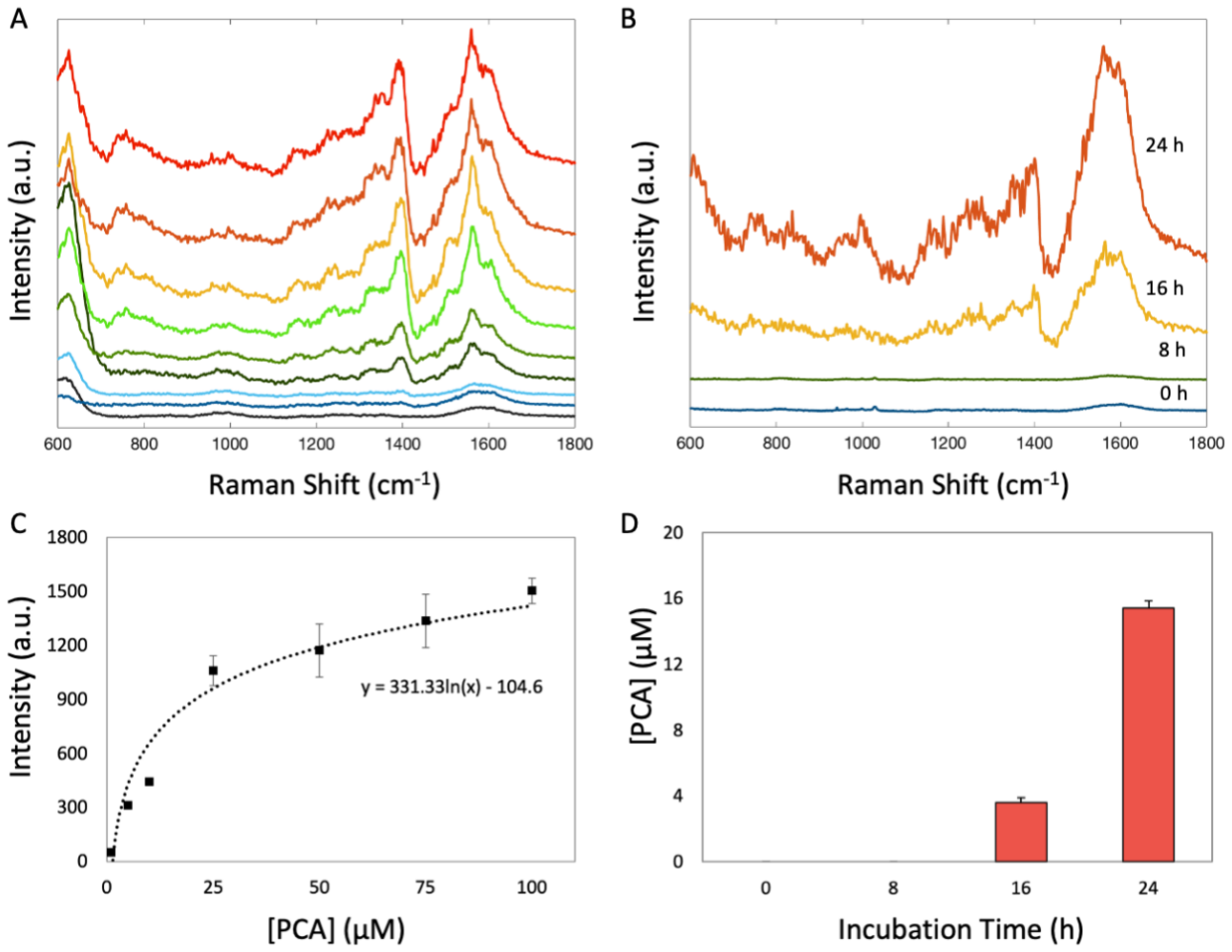

Figure 4. SERS detection of PCA. (A) SERS spectra of PCA in DI water at pH 4.5 at different concentrations (from bottom to top: 0, 100 nM, 1 µM, 5 µM, 10 µM, 25 µM, 50 µM, 75 µM, 100 µM). (B) SERS spectra of PCA produced by *P. aeruginosa* grown in planktonic cultures as a function of incubation time. (C) SERS intensity (at 1396 cm^{-1}) as a function of PCA concentration (1 µM, 5 µM, 10 µM, 25 µM, 50 µM, 75 µM, 100 µM). Dashed line is a logarithmic fit in the quantitative detection regions. The mean values and standard deviations were calculated from three independent measurements. (D) Histograms of measured PCA concentrations obtained from bacterial-free supernatant of *P. aeruginosa* cultures determined using the PCA calibration plot in panel (C) as a function of incubation time. Error bars indicate standard deviation.

For Table of Contents Use Only

Actively Controllable Solid Phase Microextraction in a Hierarchically Organized Block Copolymer-Nanopore Electrode Array Sensor for Charge-Selective Detection of Bacterial Metabolites

Jin Jia†, Seung-Ryong Kwon†, Seol Baek, Vignesh Sundaresan, Tianyuan Cao, Allison R. Cutri, Kaiyu Fu, Bridget Roberts, Joshua D. Shrout, Paul W. Bohn*

Cross-sectional SEM image and schematic illustration of the electrochemical SERS sensor with BCP gate closed at pH 7.0 (middle) and BCP gate open at pH 4.5 (right) for the permselective transport and detection of negatively charged molecules by square wave voltammetry and SERS.

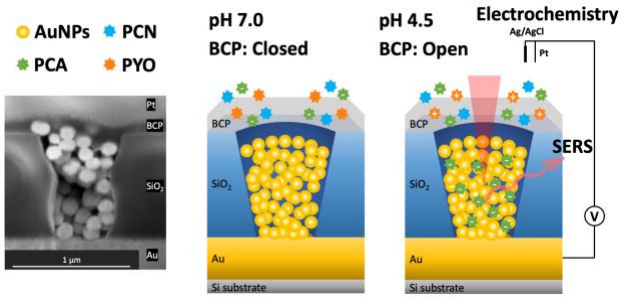

Supporting Information

Actively Controllable Solid Phase Microextraction in a Hierarchically Organized Block Copolymer-Nanopore Electrode Array Sensor for Charge-Selective Detection of Bacterial Metabolites

Jin Jia[1†], Seung-Ryong Kwon[2†], Seol Baek[1], Vignesh Sundaresan[3], Tianyuan Cao[1], Allison R. Cutri[1], Kaiyu Fu[4,5], Bridget Roberts[3], Joshua D. Shrout[6,7], Paul W. Bohn[1,3]*

[1] Department of Chemistry and Biochemistry, University of Notre Dame, Notre Dame, Indiana 46556, United States

[2] Department of Chemistry and Research Institute of Natural Science, Gyeongsang National University, Jinju, 52828, South Korea

[3] Department of Chemical and Biomolecular Engineering, University of Notre Dame, Notre Dame, Indiana 46556, United States

[4] Department of Electrical Engineering, Stanford University, Stanford, California 94305, United States

[5] Department of Radiology, Stanford University, Stanford, California 94305, United States

[6] Department of Civil and Environmental Engineering and Earth Sciences, University of Notre Dame, Notre Dame, Indiana 46556, United States

[7] Department of Biological Sciences, University of Notre Dame, Notre Dame, Indiana 46556, United States

[*]Author to whom correspondence should be addressed, *pbohn@nd.edu*.

Table of Contents

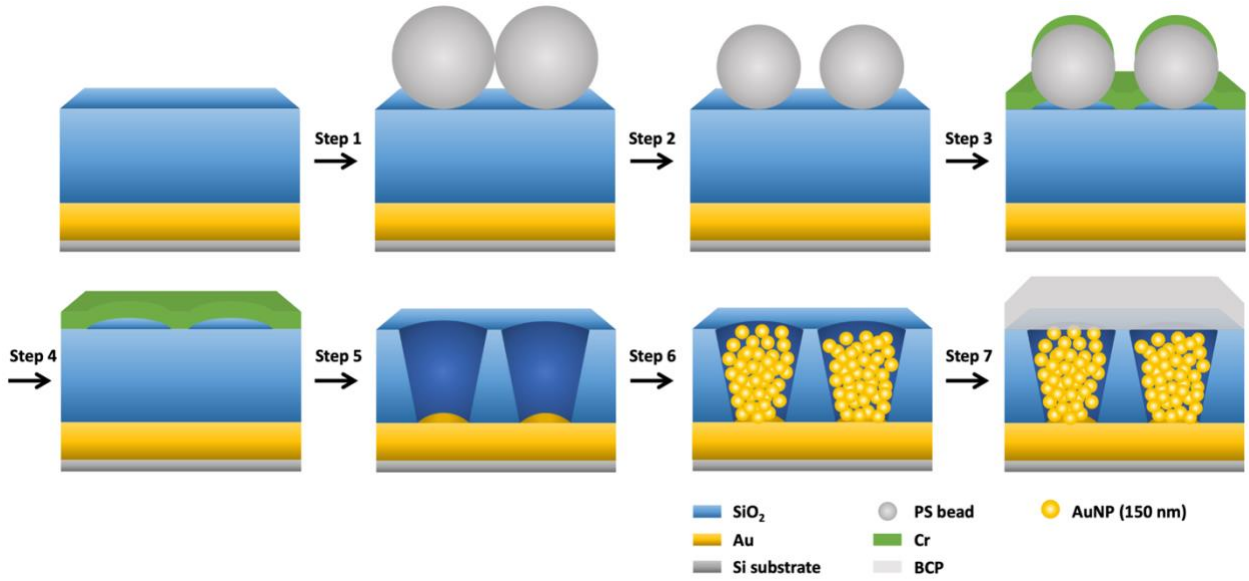

Figure S1. Electrochemical SERS sensor fabrication. (1) Deposition of a polystyrene (PS) bead close-packed monolayer. (2) Reactive ion etching (RIE) to reduce the size of the PS beads. (3) Coating with Cr etch mask. (4) Removal of the PS beads. (5) Removal of the Cr etch mask and RIE etching of the SiO_2. (6) Deposition of the Au nanoparticle SERS-enhancing medium in the nanopores. (7) Addition of the PS-*b*-P4VP BCP membrane.

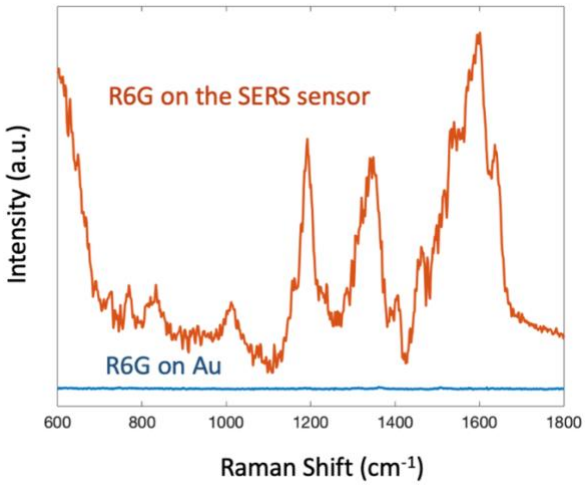

Figure S2. Representative SERS and Raman spectra of 10 mM Rhodamine 6G on the electrochemical SERS sensor (orange) and gold substrate (blue).

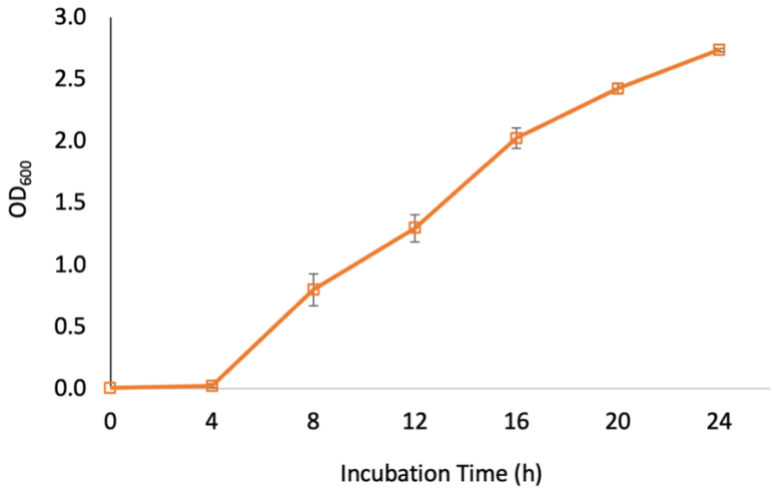

Figure S3. Growth curve of *P. aeruginosa* made by measuring OD_{600} of the liquid culture as a function of time.

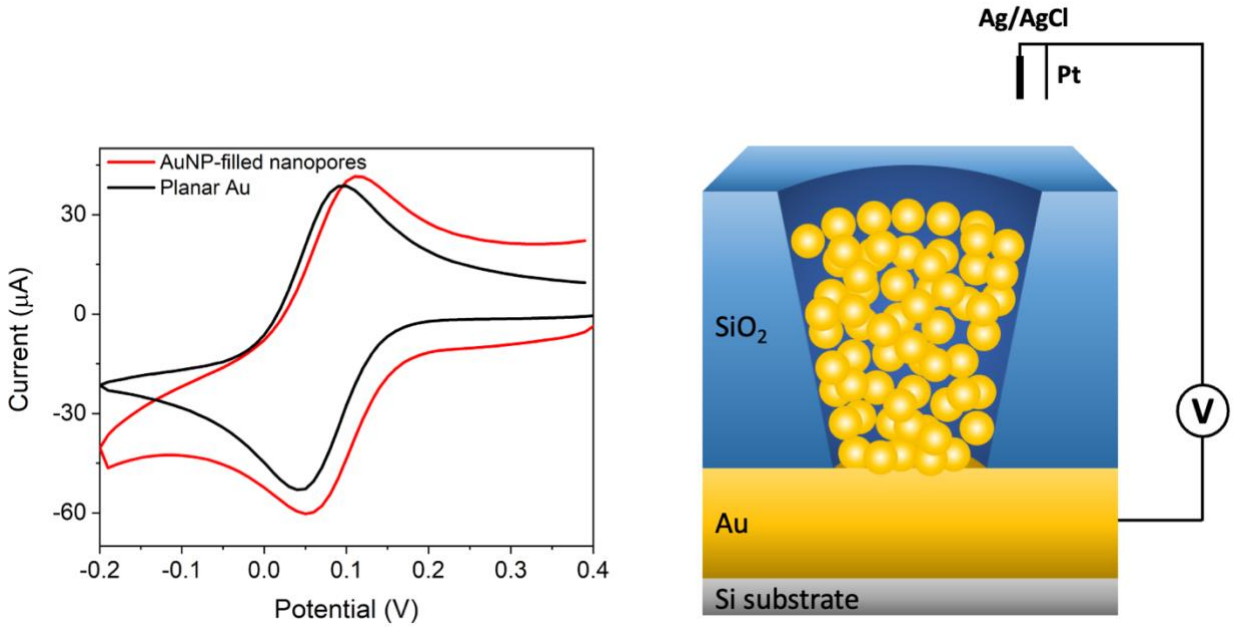

Figure S4. (*Left*) Cyclic-voltammetry of 1 mM $Fe(CN)_6^{3/4-}$ in 1 M KCl at pH 7.4 on AuNP-filled NEAs and a planar gold electrode. (*Right*) Schematic diagram showing the cross-section of a single AuNP-filled NEA nanopore. Both CVs were recorded at 100 mV s^{-1} *vs.* Ag/AgCl.

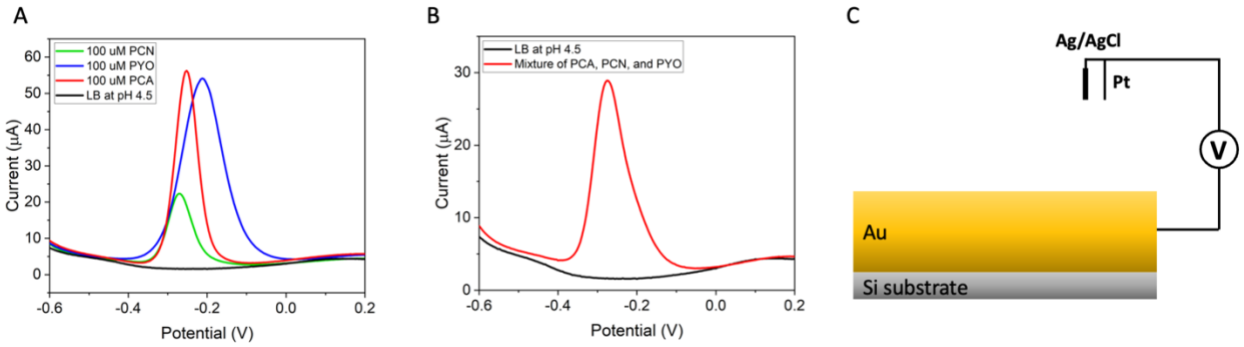

Figure S5. (A) Oxidative square wave voltammograms (SWV) of 100 µM PCA (red), 100 µM PCN (green), 100 µM PYO (blue) in LB medium at pH 4.5, and LB medium at pH 4.5 (black), respectively. (B) Oxidative SWV of a mixture containing 33.3 µM each of PCA, PCN, and PYO in LB medium at pH 4.5 (red), and LB medium alone at pH 4.5 (black). All measurements were conducted on an electrochemical cell formed from a PDMS well (6 mm diam.) mounted on a planar gold electrode.

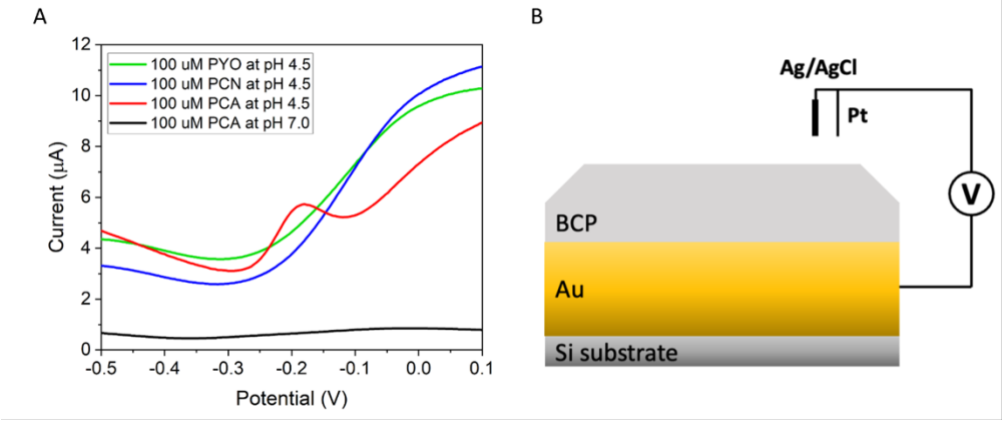

Figure S6. (A) Oxidative SWV of 100 μM PCA at pH 4.5 (red), 100 μM PCA at pH 7.0 (black), 100 μM PCN (blue) at pH 4.5, and 100 μM PYO (green) at pH 4.5 in LB medium on BCP-coated planar gold electrode. (B) BCP coated gold electrode setting. All measurements were conducted on PDMS well (6 mm in diameter)-mounted planar gold electrode.

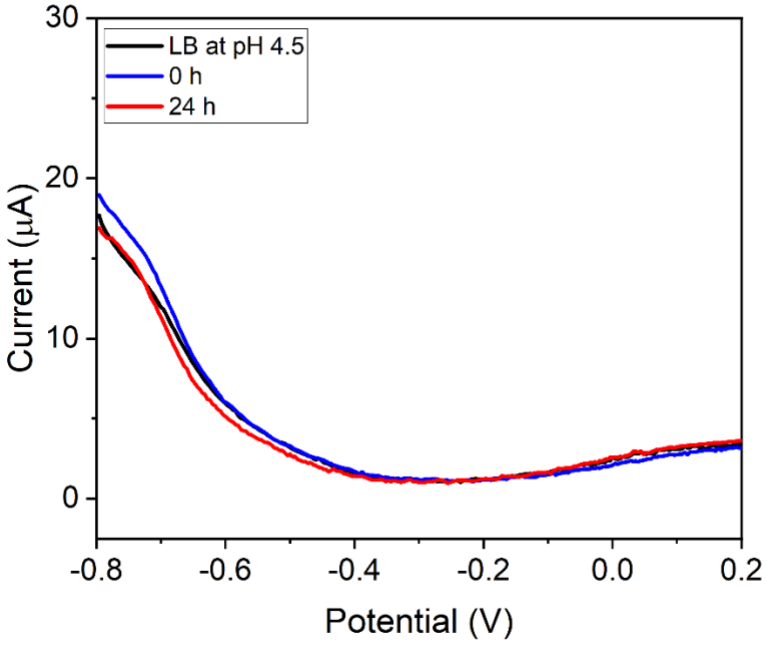

Figure S7. Oxidative square wave voltammograms (SWV) obtained at different incubation times (from 0 to 24 h) from *P. aeruginosa* Δ*phz* grown in LB medium at pH 4.5 on a planar gold electrode.

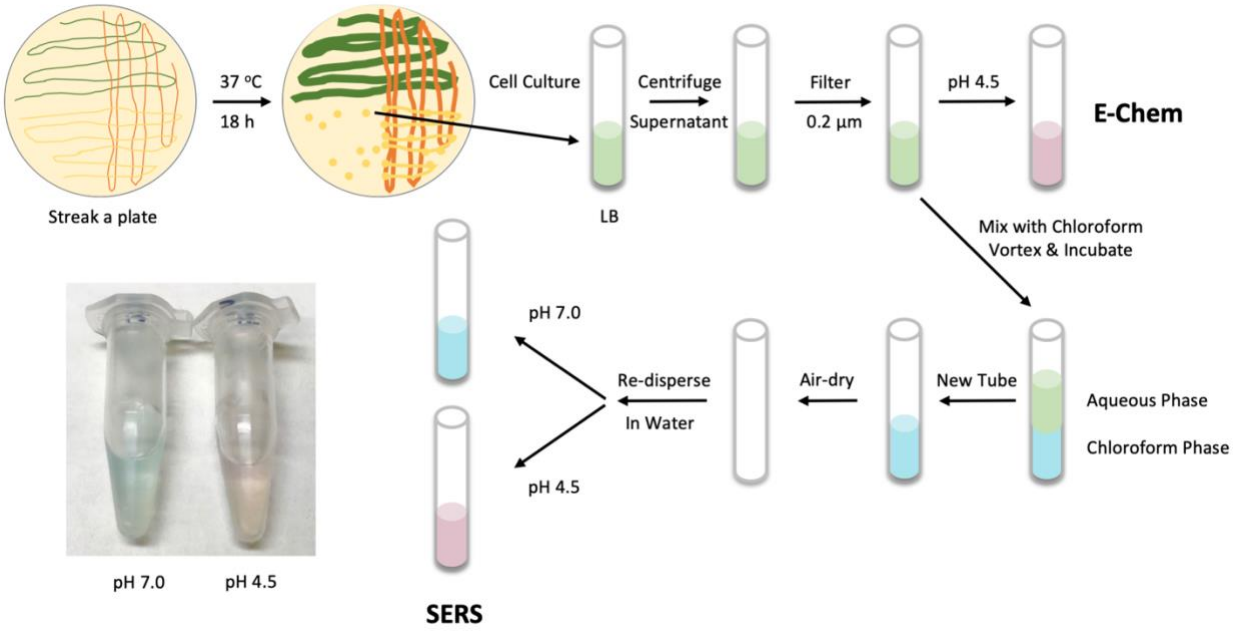

Figure S8. The preparation process of the *P. aeruginosa*-free supernatant for electrochemical testing and SERS testing.

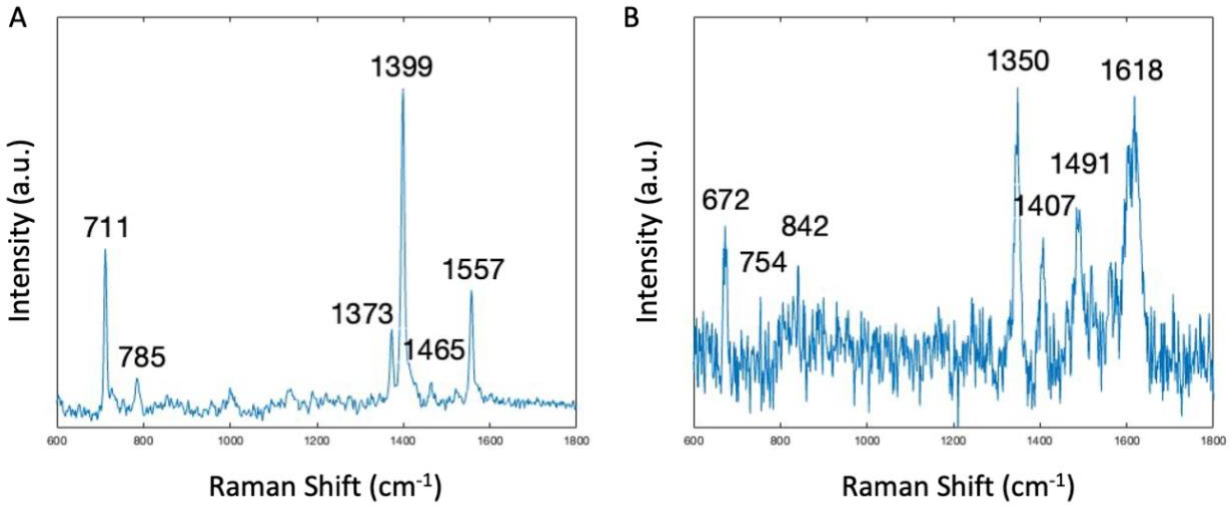

Figure S9. Raman spectra of PCN (A) and PYO (B) on gold.

Table S1. Raman standard band positions.

Compounds	Raman Standard Band Positions (cm^{-1})
PCA Standard	626, 758, 1146, 1227, 1337, 1396, 1472, 1559
PCN Standard	711, 785, 1373, 1399, 1465, 1557
PYO Standard	672, 754, 842, 1350, 1407, 1491, 1618